Available online at www.sciencedirect.com
ScienceDirect
Pattern Recognition 41 (2008) 117–129
PATTERN RECOGNITION
THE JOURNAL OF THE PATTERN RECOGNITION SOCIETY
www.elsevier.com/locate/pr

A novel image thresholding method based on Parzen window estimate

Shitong Wang[a,b,*], Fu-lai Chung[b], Fusong Xiong[a]

[a]*School of Information, Southern Yangtse University, WuXi, JiangSu, China*
[b]*Department of Computing, Hong Kong Polytechnic University, Hong Kong, China*

Received 8 March 2006; received in revised form 23 March 2007; accepted 29 March 2007

Abstract

Image segmentation is one of the most important and fundamental tasks in image processing and techniques based on image thresholding are typically simple and computationally efficient. However, the image segmentation results depend heavily on the chosen image thresholding methods. In this paper, histogram is integrated with the Parzen window technique to estimate the spatial probability distribution of gray-level image values, and a novel criterion function is designed. By optimizing the criterion function, an optimal global threshold is obtained. The experimental results for synthetic real-world and images demonstrate the success of the proposed image thresholding method, as compared with the OTSU method, the MET method and the entropy-based method.

Keywords: Parzen window; Thresholding; Image segmentation

1. Introduction

Image segmentation involves subdividing an image into its constituent parts and extracting them accordingly [1,2]. Image segmentation by thresholding is the simplest technique which involves the basic assumption that the objects and backgrounds in an image have distinct gray-level distributions. This assumption implies that the gray values contain two or more distinct peaks and there exists a threshold value separating them. Thus, by assigning regions having gray levels below the threshold as backgrounds and assigning those regions having gray levels above the threshold as objects, or conversely by assigning regions having gray levels above the threshold as backgrounds and assigning those regions having gray levels below the threshold as objects, the segmentation task can be performed. There are two types of thresholding methods [3–22,32,34], i.e., global thresholding and local thresholding. As the global thresholding methods are easy to be implemented and also computationally less involved, they are our main concern in this paper.

Many global thresholding techniques have been developed over the past years to segment images and recognize patterns, for typical examples, OTSU method [23], minimum error thresholding (MET) method [24], maximum cross entropy method (referred as entropy-based method in this paper) [25,26] and Tsallis entropy-based method [27]. By using the gray-level histogram which is an approximation of the gray-level probability density function, the MET method, proposed by Kittler and Illingworth in 1986, is suitable for such images in which the object to background ratio is less then $1:10^2$. By maximizing the variance between the objects and backgrounds in an image, the OTSU method, proposed by Otsu in 1979, can dynamically determine the threshold. Thus, it is a good thresholding method for most images. The maximum cross entropy methods are also effective for images with different signal-to-noise ratios and different objects. All the above methods are rooted at the gray-level histogram of an image, which is used to approximate the unknown gray-level probability density function.

This paper attempts to explore a novel global image thresholding method which is rooted at the Parzen window estimate of the unknown gray value probability density function rather than the gray-level histograms of an image. The Parzen window estimate effectively integrates image histogram information

* Corresponding author. School of Information, Southern Yangtse University, WuXi, JiangSu, China. Tel.: +86 510 85912151.
E-mail address: wxwangst@yahoo.com.cn (S. Wang).

0031-3203/$30.00
doi:10.1016/j.patcog.2007.03.029

with the *explicit* spatial information about pixels of different gray levels. The MHUE thresholding method [28] also utilizes the spatial information of image. However, the spatial information is *implicitly* represented in this method, by an image morphology-based property called *region homogeneity*. Comparing with the OTSU method, the MET method and the entropy-based methods, the performance of our image thresholding method, as indicated by the experimental results, is particularly attractive in image segmentation quality, even for images with multipeaks in their gray-level histograms. The remainder of this paper is organized as follows. In Section 2, the Parzen window estimate method for images is briefly reviewed. In Section 3, we propose our novel image thresholding method. In Section 4, the experimental results are presented and discussed. The final section concludes the paper.

2. Parzen window estimate for images

The Parzen window estimate [29–31] is a very traditional and effective non-parametric estimation approach. Here, we briefly introduce the involved concept.

Assume $f(x, y)$ be the gray value of the pixel located at the point (x, y). In an image $\{f(x, y)|x \in \{1, 2, \ldots, m\}, y \in \{1, 2, \ldots, n\}\}$ of size $N = m \times n$ with L gray levels, let $\omega_i = \{(x, y)|f(x, y) = i, x \in \{1, 2, \ldots, m\}, y \in \{1, 2, \ldots, n\}, i \in \{1, 2, \ldots, L\}\}$, and C_i denote the number of points in ω_i, $i = 1, 2, \ldots, L$, then $N = \sum_{i=1}^{L} C_i$. Obviously, ω_i is defined in a two-dimensional space. According to the Parzen window technique, for the point space ω_i, its probability density function $p(x, y, \omega_i)$ can be approximated using the following formulas:

$$p(x, y|\omega_i) = \frac{1}{C_i} \sum_{j=1}^{C_i} \frac{1}{V_{C_i}} \varphi(x, y; x_j, y_j; h_{C_i}^2), \tag{1}$$

$$\begin{aligned} p(x, y, \omega_i) &= p(\omega_i) p(x, y|\omega_i) \\ &= \frac{C_i}{N} \cdot \frac{1}{C_i} \sum_{j=1}^{C_i} \frac{1}{V_{C_i}} \varphi(x, y; x_j, y_j; h_{C_i}^2) \\ &= \frac{1}{N} \cdot \sum_{j=1}^{C_i} \frac{1}{V_{C_i}} \varphi(x, y; x_j, y_j; h_{C_i}^2), \end{aligned} \tag{2}$$

where h_{C_i} denotes the window width of the ith gray-level set, (x_j, y_j) denotes the jth pixel in ω_i, V_{C_i} denotes the volume of the corresponding cube with h_{C_i} as its length of each edge, i.e., $V_{C_i} = h_{C_i}^2$ for an image; $p(\omega_i)$ can be approximated by C_i/N, $1 \leqslant i \leqslant L$, and $\varphi(\cdot)$ is a kernel function. In this paper, the following Gaussian function for $\varphi(\cdot)$ is taken:

$$\varphi(x, y; x_j, y_j; h_{C_i}^2) = \frac{1}{2\pi} \exp\left(-\frac{(x - x_j)^2 + (y - y_j)^2}{2h_{C_i}^2}\right). \tag{3}$$

Thus, for any pixel (x, y) in the above image, its probability density function $p(x, y)$ can be estimated using

$$\begin{aligned} p(x, y) &= \sum_{i=1}^{L} p(x, y, \omega_i) = \sum_{i=1}^{L} p(\omega_i) p(x, y|\omega_i) \\ &= \frac{1}{N} \sum_{i=1}^{L} \sum_{j=1}^{C_i} \frac{1}{V_{C_i}} \varphi(x, y; x_j, y_j; h_{C_i}^2) \\ &= \frac{1}{2\pi N} \sum_{i=1}^{L} \sum_{j=1}^{C_i} \frac{1}{h_{C_i}^2} \\ &\quad \times \exp\left(-\frac{(x - x_j)^2 + (y - y_j)^2}{2h_{C_i}^2}\right). \end{aligned} \tag{4}$$

In general, as pointed in Refs. [29,30], h_{C_i} should assure that

$$\lim_{C_i \to \infty} V_{C_i} = 0, \quad \lim_{C_i \to \infty} C_i V_{C_i} = \infty. \tag{5}$$

In most cases, taking V_{C_i} as $1/\sqrt{C_i}$ is a good choice [29,30], i.e., $V_{C_i} = h_{C_i}^2 = 1/\sqrt{C_i}$. In this study, $h_{C_i} = (1/C_i)^{1/4}$ is taken. As we may know well, when the Parzen window estimate is used for images, it implicitly assumes the spatial compactness of every gray level. This may not hold true for some gray levels in which their C_i's are comparatively small, or all the data points are sparsely scattered. An effective solution strategy for such a gray level is to unite it together with its adjacent gray levels into a new gray level such that the spatial compactness of every gray level can be basically achieved. In this study, this strategy is taken when C_i for the ith gray level is small.

3. The proposed image thresholding method

As we may know well, the optimal threshold can be determined by optimizing a suitable criterion function obtained from the gray value distribution of the image and some other features of the image. Let t be a threshold. The result of thresholding an image of size $m \times n$ at gray level t is to separate all gray levels into two classes, i.e., the background class (denoted as class p for simplicity) and the object class (denoted as class r here):

$$\boldsymbol{p} : \omega_1, \omega_2, \ldots, \omega_t, \quad 1 \leqslant t < L, \tag{6}$$

$$\boldsymbol{r} : \omega_{t+1}, \omega_{t+2}, \ldots, \omega_L. \tag{7}$$

Thus, these two classes constitute the corresponding probability spaces and their probability density function $p(x, y)$ and $r(x, y)$ can be formulated as follows using the Parzen window estimate:

$$\begin{aligned} p(x, y) &= \frac{1}{N} \sum_{i=1}^{t} \sum_{j=1}^{C_i} \frac{1}{V_{C_i}} \varphi(x, y; x_j, y_j; h_{C_i}^2) \\ &= \frac{1}{2\pi N} \sum_{i=1}^{t} \sum_{j=1}^{C_i} \frac{1}{h_{C_i}^2} \\ &\quad \times \exp\left(-\frac{(x - x_j)^2 + (y - y_j)^2}{2h_{C_i}^2}\right), \end{aligned} \tag{8}$$

$$r(x,y)=\frac{1}{N}\sum_{i=t+1}^{L}\sum_{j=1}^{C_i}\frac{1}{V_{C_i}}\varphi(x,y;x_j,y_j;h_{C_i}^2)$$

$$=\frac{1}{2\pi N}\sum_{i=t+1}^{L}\sum_{j=1}^{C_i}\frac{1}{h_{C_i}^2}\times\exp\left(-\frac{(x-x_j)^2+(y-y_j)^2}{2h_{C_i}^2}\right). \quad (9)$$

In general, a thresholding method determines the optimal gray value t_{opt} of t based on a certain criterion function. In order to achieve this goal, we should choose t_{opt} such that the class p and the class r can be well separated. Here, we adopt the following criterion function in our study:

$$t_{opt}=\arg\max_t\int\int_{\Omega}(p(x,y)-r(x,y))^2\,\mathrm{d}x\,\mathrm{d}y, \quad (10)$$

i.e.,

$$t_{opt}=\arg\max_t\int\int_{\Omega}(p(x,y)-r(x,y))^2\,\mathrm{d}x\,\mathrm{d}y$$

$$=\int\int_{\Omega}p^2(x,y)\,\mathrm{d}x\,\mathrm{d}y+\int\int_{\Omega}r^2(x,y)\,\mathrm{d}x\,\mathrm{d}y-2\int\int_{\Omega}p(x,y)r(x,y)\,\mathrm{d}x\,\mathrm{d}y, \quad (11)$$

where $\Omega=[1,m]\times[1,n]$.

Next, let us derive $\int\int_{\Omega}p^2(x,y)\,\mathrm{d}x\,\mathrm{d}y$, $\int\int_{\Omega}r^2(x,y)\,\mathrm{d}x\,\mathrm{d}y$ and $\int\int_{\Omega}p(x,y)r(x,y)\,\mathrm{d}x\,\mathrm{d}y$ using the following important results [31]:

$$\int_D G(\mathbf{x},\mathbf{x}_i,\sigma_1^2)G(\mathbf{x},\mathbf{x}_j,\sigma_2^2)\,\mathrm{d}\mathbf{x}=G(\mathbf{x}_i,\mathbf{x}_j,\sigma_1^2+\sigma_2^2), \quad (12)$$

$$\int_D\sum_{i=1}^{N_1}\sum_{j=1}^{N_2}G(\mathbf{x},\mathbf{x}_i,\sigma_1^2)G(\mathbf{x},\mathbf{x}_j,\sigma_2^2)\,\mathrm{d}\mathbf{x}=\sum_{i=1}^{N_1}\sum_{j=1}^{N_2}G(\mathbf{x}_i,\mathbf{x}_j,\sigma_1^2+\sigma_2^2), \quad (13)$$

where for some data space D, with $\mathbf{x},\mathbf{x}_i,\mathbf{x}_j\in D$, $G(\mathbf{x},\mathbf{x}_i,\sigma_1^2)$, $G(\mathbf{x},\mathbf{x}_j,\sigma_2^2)$ are defined by the following Gaussian kernel functions:

$$G(x,x_i,\sigma_1^2)=\frac{1}{\sigma_1^2}\varphi(x,x_i,\sigma_1^2), \quad (14)$$

$$G(x,x_j,\sigma_2^2)=\frac{1}{\sigma_2^2}\varphi(x,x_j,\sigma_2^2). \quad (15)$$

By substituting (8) and (9) into (11), we have

$$\int\int_{\Omega}p^2(x,y)\,\mathrm{d}x\,\mathrm{d}y$$

$$=\frac{1}{N^2}\int\int_{\Omega}\left(\sum_{i=1}^{t}\sum_{j=1}^{C_i}\frac{1}{h_{C_i}^2}\varphi(x,y;x_j,y_j;h_{C_i}^2)\right)^2\mathrm{d}x\,\mathrm{d}y$$

$$=\frac{1}{N^2}\int\int_{\Omega}\left(\sum_{i=1}^{t}\sum_{j=1}^{C_i}G(x,y;x_j,y_j;h_{C_i}^2)\right)^2\mathrm{d}x\,\mathrm{d}y$$

$$=\frac{1}{N^2}\sum_{i=1}^{t}\sum_{j=1}^{C_i}\sum_{l=1}^{t}\sum_{k=1}^{C_l}\int\int_{\Omega}G(x,y;x_j,y_j;h_{C_i}^2)\times G(x,y;x_k,y_k;h_{C_l}^2)\,\mathrm{d}x\,\mathrm{d}y$$

$$=\frac{1}{N^2}\sum_{i=1}^{t}\sum_{j=1}^{C_i}\sum_{l=1}^{t}\sum_{k=1}^{C_l}G(x_j,y_j;x_k,y_k;h_{C_i}^2+h_{C_l}^2). \quad (16)$$

Similarly, we have

$$\int\int_{\Omega}r^2(x,y)\,\mathrm{d}x\,\mathrm{d}y=\frac{1}{N^2}\sum_{i=t+1}^{L}\sum_{j=1}^{C_i}\sum_{l=t+1}^{L}\sum_{k=1}^{C_l}\times G(x_j,y_j;x_k,y_k;h_{C_i}^2+h_{C_l}^2), \quad (17)$$

$$\int\int_{\Omega}p(x,y)r(x,y)\,\mathrm{d}x\,\mathrm{d}y=\frac{1}{N^2}\sum_{i=1}^{t}\sum_{j=1}^{C_i}\sum_{l=t+1}^{L}\sum_{k=1}^{C_l}G(x_j,y_j;x_k,y_k;h_{C_i}^2+h_{C_l}^2). \quad (18)$$

By substituting (16)–(18) into (11), a novel criterion function can be obtained. Thus, we can find an optimal gray value t_{opt} using the following Parzen-Window based Thresholding (PWT) procedure:

Procedure *PWT*.
BEGIN
1. For a given image f of size $N=m\times n$ with L gray levels, construct the gray-level histogram from the given image.
2. Initialize $t(1:L-1)=0$;
3. For $\boldsymbol{i}=1:\boldsymbol{L}-1$
   Begin
   3.1 Compute $\int\int_{\Omega}p^2(x,y)\,\mathrm{d}x\,\mathrm{d}y$, $\int\int_{\Omega}r^2(x,y)\,\mathrm{d}x\,\mathrm{d}y$, and $\int\int_{\Omega}p(x,y)r(x,y)\,\mathrm{d}x\,\mathrm{d}y$ using (16)–(18), respectively.
   3.2 $t(i)=\int\int_{\Omega}p^2(x,y)\,\mathrm{d}x\,\mathrm{d}y+\int\int_{\Omega}r^2(x,y)\,\mathrm{d}x\,\mathrm{d}y-2\int\int_{\Omega}p(x,y)r(x,y)\,\mathrm{d}x\,\mathrm{d}y$
   End
4. t_{opt}=min(t); /* choose the minimum from all $\boldsymbol{t(i)}|\boldsymbol{i}=1,2,\ldots,\boldsymbol{L}-1$*/
5. Segment the image using the threshold value $\boldsymbol{t}_{opt}$, and output the segmented image accordingly.

END

4. Experimental results

In this section, we report the experimental results obtained using the proposed method. In order to assess the effectiveness of the proposed thresholding method, several synthetic and real images including some non-destructive testing (NDT) images were used in the experiments. The results provided by the proposed method were compared with those yielded by three thresholding techniques widely used in the literature, i.e., the OTSU method [23], the MET method [24] and entropy-based method [25]. The latest advance in image thresholding research is the Tsallis entropy-based method [27]. As we have proved the equivalence relationship between the entropy-based method and the Tsallis entropy-based image thresholding in Ref. [33], a comparison with the Tsallis entropy-based method is omitted here. At present, there are several measures [35,36,39] which may be used in the evaluation of the effectiveness of image thresholding methods. In this study, we employ misclassification error (ME) measure [35] to evaluate the performances of these thresholding methods. Considering image segmentation as a pixel classification process, the percentage of pixel misclassification is the discrepancy measure that comes most readily to mind. ME reflects the percentage of background pixels wrongly assigned to foreground, and conversely, foreground pixels wrongly assigned to background. For the two-class segmentation problem, ME can be simply expressed as

$$ME = 1 - \frac{|B_O \cap B_T| + |F_O \cap F_T|}{|B_O| + |F_O|}, \tag{19}$$

where B_O and F_O denote the background and foreground of the ground-truth image, respectively; B_T and F_T denote the background and foreground area pixels in the test image, respectively, and $|\bullet|$ is the cardinality of the set $\bullet$. The ME varies from 0 for a perfectly classified image to 1 for a totally wrongly classified image.

4.1. Experiment on synthetic image

It is usually desirable to test the thresholding algorithm using the synthetic images for which the ideal threshold(s) can be identified directly [37]. As shown in Fig. 1(a), original image with 256 × 256 pixels shows some round gray objects (with level 150) on the darker background (with level 50). Ideal segmentation is shown in Fig. 1(b). Gaussian noise is added to the original image. Fig. 1(c) is an example of the noise image and its histogram is shown in Fig. 1(d). Obviously, Fig. 1(c) shows a synthetic noise image with two components. Table 1 lists the results in terms of threshold values, of number of misclassified pixels, of ME and of running times obtained by applying each thresholding method to the noise image Fig. 1(c). The optimal threshold (found by manually thresholding the image on the basis of the information present in the ideal thresholded image Fig. 1(b)) is at 101 (the valley of the histogram). The threshold by the proposed method is exactly the valley (corresponding to 61 misclassified pixels and its ME equal to 9.3097e − 004), whereas that by the entropy-based method is 77 (corresponding to 1835 misclassified pixels and its ME equal to 0.0280), the MET method is 112 (corresponding to 247 misclassified

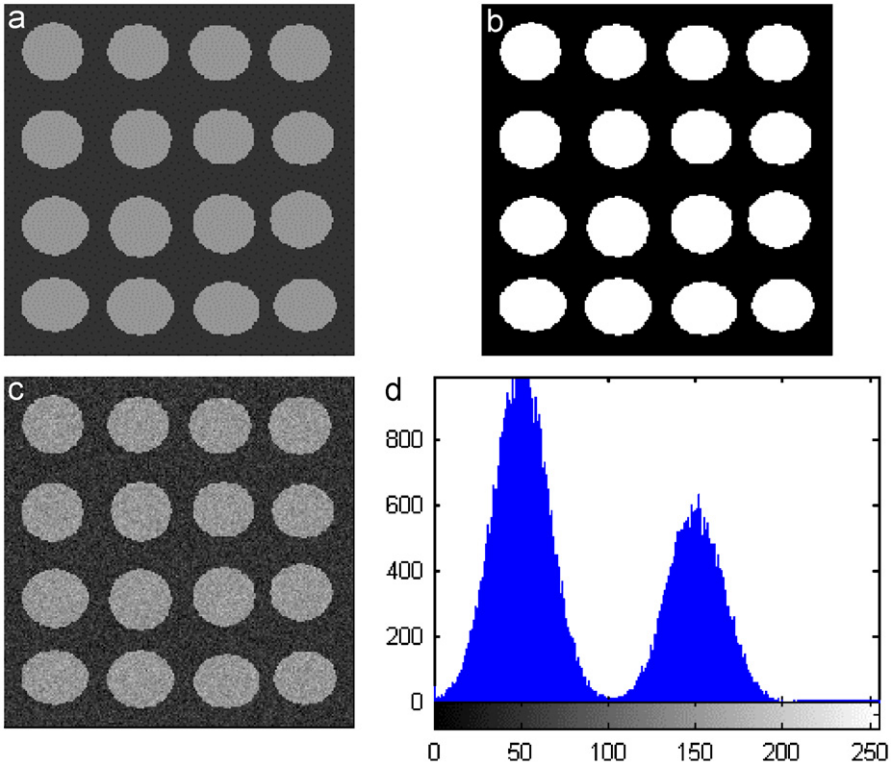

Fig. 1. Example of a test image used in the experiment simulating object and background: (a) original synthetic image, (b) ideal thresholded image, (c) noise image with Gaussian noise, (d) histogram of the noise image.

Table 1
Threshold values, numbers of misclassified pixels, MEs and running times obtained using the different thresholding methods for the synthetic image

	Optimal	MET	OTSU	Entropy-based method	The proposed method
Synthetic image					
Threshold value	101	112	97	77	101
Misclassified pixels	61	247	77	1835	61
ME	9.3079e − 004	0.0038	0.0012	0.0280	9.3079e − 004
Running time (s)		0.638	0.632	0.581	132.953

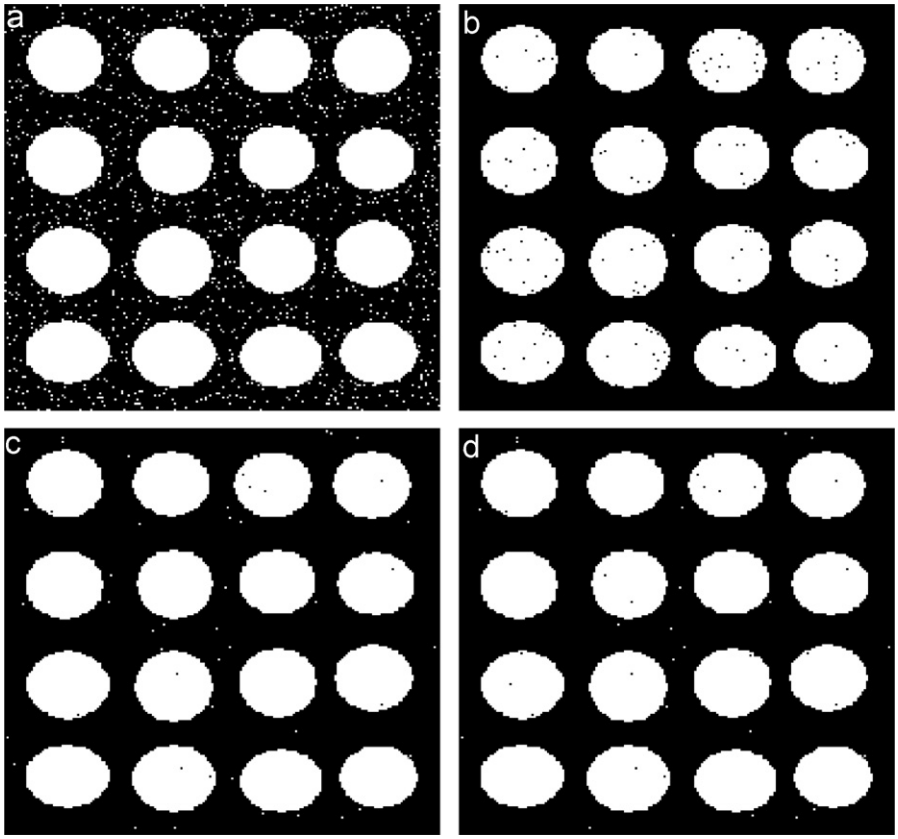

Fig. 2. A comparison for the synthetic binary image obtained using the reference thresholding techniques and the proposed method. (a) Entropy-based method ($t = 77$). (b) MET method ($t = 112$). (c) OTSU method ($t = 97$). (d) The proposed method ($t = 101$).

pixels and its ME equal to 0.0038), and the OTSU method is 97 (corresponding to 77 misclassified pixels and its ME equal to 0.0012). Among the reference thresholding techniques, the worst result was provided by the entropy-based method, which totally failed to determine a reasonable threshold, while the threshold closest to the one yielded by the proposed method was computed by OTSU method. Fig. 2 provides a visual comparison between the binary image obtained by the reference thresholding techniques and the proposed method. As can be seen from the thresholded images (Fig. 2), one can conclude that the OTSU method leads to a cleaner segmentation image which proved almost as accurate as the proposed method since it provided threshold values very close to the optimal ones. The MET method seems dealing satisfactory except for a more noise. By contrast, the entropy-based method performed almost unvalued because it misclassified too much background (noise) as the object (see Fig. 2(a)). Moreover, we should note that although the proposed method is best for the synthetic image among these four methods, it must take much more running time. When the running time of each other method is less than 1 s (see Table 1), the proposed method must take 132.953 s for the synthetic image in this experiment.

4.2. Experiments on NDT images

The second set of experiments is related to the problem of the analysis of NDT images. NDT consists of the use of special equipments and methods to detect an object and quantify its possible defects without harming it. NDT methods are used in a broad variety of applications, such as nuclear industry, chemistry, aeronautics and astronautics, civil constructions, etc. [38]. In this study, three real NDT images were used in the experi-

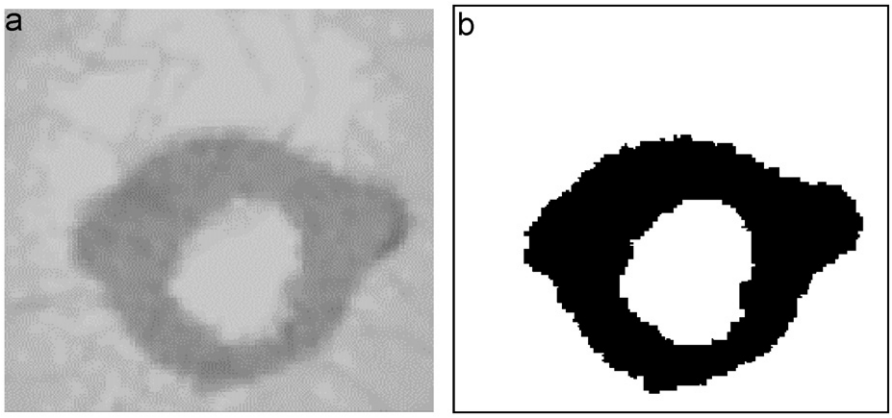

Fig. 3. First NDT: (a) eddy current image; (b) ground-truth image.

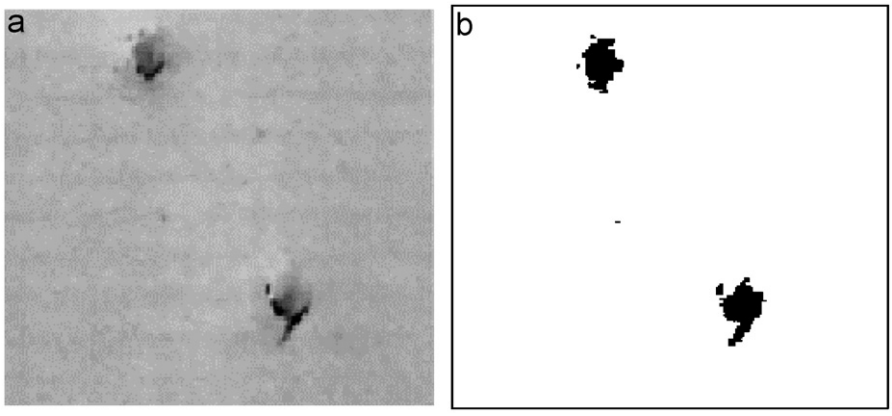

Fig. 4. Second NDT: (a) defective material image; (b) ground-truth image.

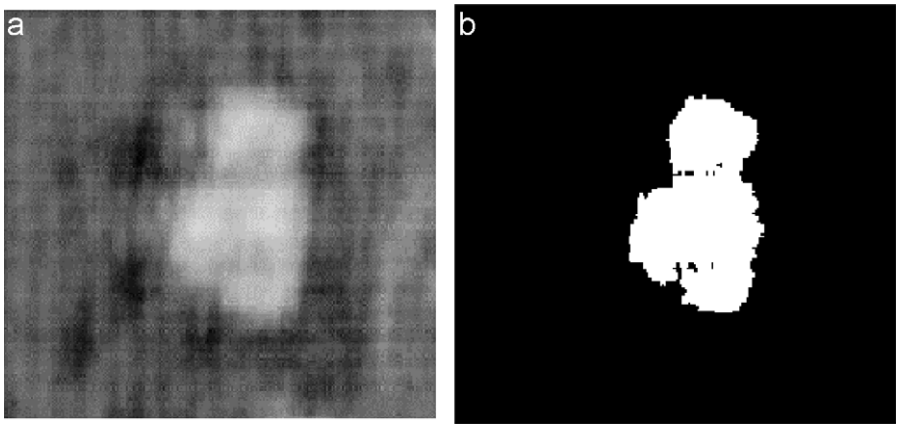

Fig. 5. Third NDT: (a) GFRP image; (b) ground-truth image.

ments to assess the performance of the proposed method. The first image represents a defective eddy current image. Eddy current image inspection is frequently used for the detection of invisible small cracks and defects of different materials including aircraft fuselages. A defective eddy current image and its ground-truth segmentation are illustrated in Figs. 3(a) and (b), where the dark region, representing the rivet surroundings, must be circular in a healthy case. The second NDT image depicts a defective fuselage material image. The original image and its corresponding ground-truth segmentation are shown in Figs. 4(a) and (b). The third NDT image depicts an ultrasonic image of a defective glass-fiber reinforced plastics (GFRP) image. The GFRP image and its corresponding ground-truth segmentation are given in Figs. 5(a) and (b).

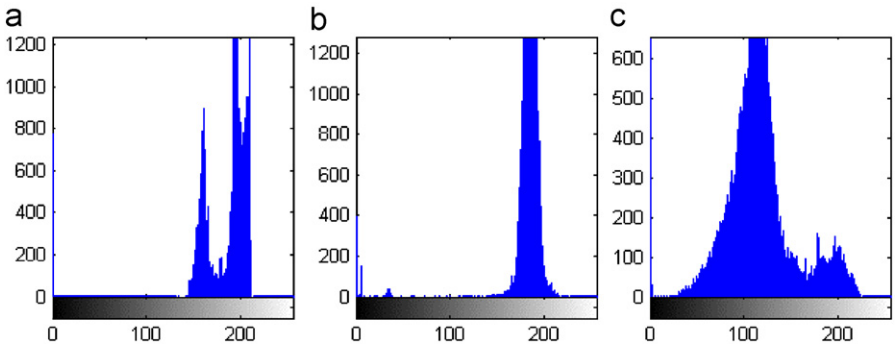

Fig. 6. Histograms of three NDT images: (a) eddy current image; (b) defective material image; (c) GFRP image.

Table 2
Threshold values, numbers of misclassified pixels, MEs and running times obtained using different thresholding methods for: (a) the eddy current image; (b) the defective material image; (c) GFRP image

	Optimal	MET	OTSU	Entropy-based method	The proposed method
(a)					
Threshold value	174	182	179	188	173
Misclassified pixels	464	995	725	2207	490
ME	0.0121	0.0259	0.0189	0.0575	0.0142
Running time (s)		0.631	0.625	0.601	118.709
(b)					
Threshold value	154	162	112	166	156
Misclassified pixels	381	497	789	641	385
ME	0.0095	0.0124	0.0197	0.0160	0.0096
Running time (s)		0.532	0.527	0.521	107.625
(c)					
Threshold value	170	174	140	138	171
Misclassified pixels	38	231	2622	2926	43
ME	9.5000e − 004	0.0058	0.0655	0.0732	0.0011
Running time (s)		0.641	0.636	0.581	129.825

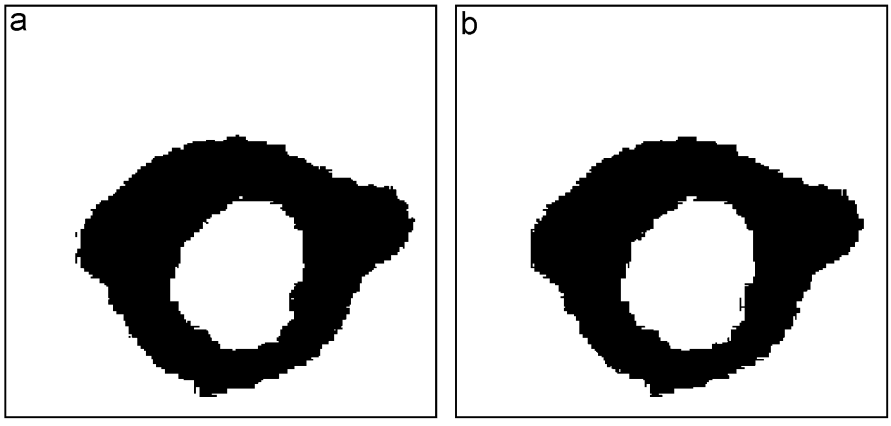

Fig. 7. NDT eddy current binary images obtained by: (a) manual supervised optimal thresholding ($t = 174$); (b) the proposed thresholding method ($t = 173$).

The results in terms of threshold values, of number of misclassified pixels, of ME and of running times obtained by applying each thresholding method to the first NDT image (whose histogram is reported in Fig. 6(a)) are reported in Table 2(a) (it is worth noting that all the pixels were assigned to one of the two classes without any rejection option). They show that the threshold value yielded by the proposed method was the closest to the optimal one. In this case, it was equal to 173, corresponding to 490 misclassified pixels and its ME equal to 0.0142, while the optimal threshold (found by manually thresholding the image on the basis of the information present in the ground-truth image) was equal to 174, corresponding to 551 misclassified pixels and its ME equal to 0.0121 (see Fig. 7 for a visual comparison between the binary image obtained by

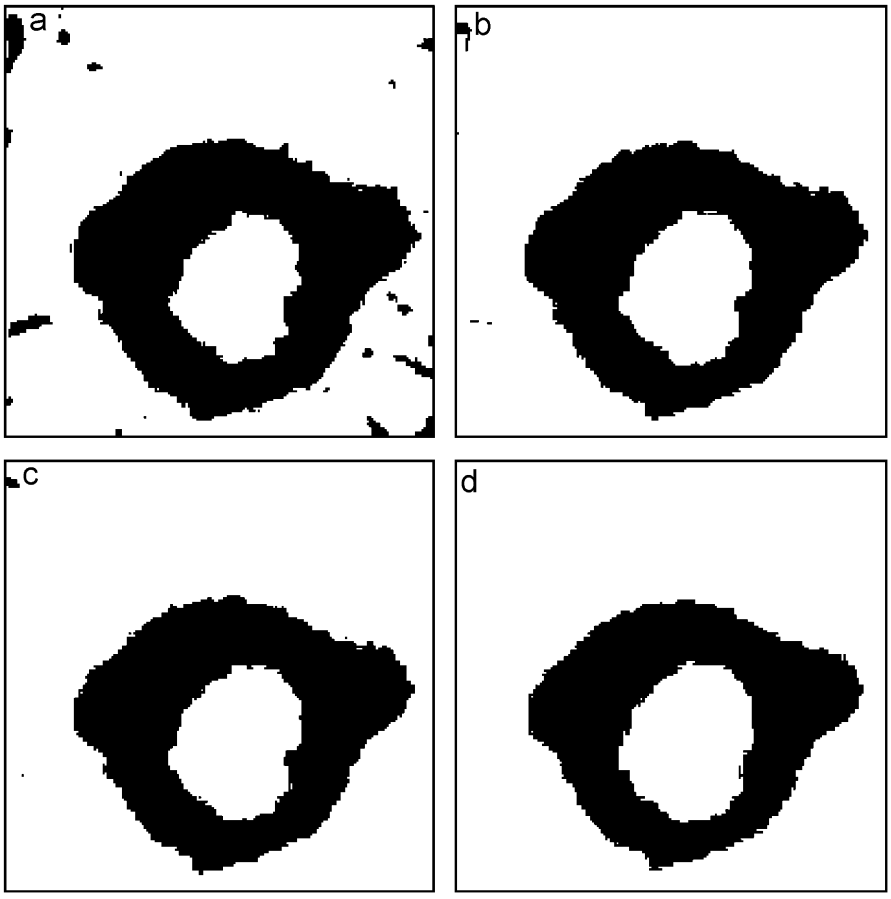

Fig. 8. A comparison for the NDT eddy current binary images obtained by the reference thresholding techniques and the proposed method. (a) Entropy-based method ($t = 188$). (b) MET method ($t = 182$). (c) OTSU method ($t = 179$). (d) The proposed method ($t = 173$).

the proposed method and the one yielded by manual optimal thresholding). Among the reference thresholding techniques, the worst result was provided by the entropy-based method (the threshold value was equal to 188, corresponding to 2207 misclassified pixels and its ME equal to 0.0575), which failed to determine a reasonable threshold, while the threshold closest to the one yielded by the proposed method was computed by the OTSU method (the threshold value was equal to 179, corresponding to 725 misclassified pixels and its ME equal to 0.0189). Fig. 8 provides a visual comparison between the binary image obtained by the reference thresholding techniques and the proposed method. Besides, just like in the experiment on synthetic image, the proposed method occupied much more running time for these three NDT images. When the running time of each other method is less than 1 s (see Table 2), the proposed method occupied 118.709, 107.625, 129.825 s for the eddy current image, the defective material image and the GFRP image, respectively. Therefore, how to greatly reduce the running time of the proposed method is an interesting topic worthy to be studied in future.

The results obtained by thresholding the histogram (see Fig. 6(b)) of the defective material image are provided in Table 2(b). In this case, the best threshold value was given by the proposed method. It was equal to 156, corresponding to 385 misclassified pixels and its ME equal to 0.0096, while the optimal threshold obtained by manual supervised thresholding was equal to 154, corresponding to 385 misclassified pixels and its ME equal to 0.0095. This promising result is confirmed by visually inspecting the binary images obtained both by the proposed method and by manual optimal thresholding (see Fig. 9). Among the reference thresholding techniques, the worst result was provided by the OTSU method (the threshold value was equal to 112, corresponding to 789 misclassified pixels and its ME equal to 0.0197), which failed to determine a reasonable threshold, while the threshold closest to the one yielded by the proposed method was computed by the MET method (the threshold value was equal to 162, corresponding to 497 misclassified pixels and its ME equal to 0.0124). Fig. 10 provides a visual comparison between the binary image obtained by the reference thresholding techniques and the proposed method.

The results obtained by thresholding the third NDT GFRP image (its histogram is reported in Fig. 6(c)) are reported in Table 2(c). Also in this case, the threshold value yielded by the proposed method was the closest to the optimal one. It was equal to 171, corresponding to 43 misclassified pixels and its ME equal to 0.0011, while the optimal threshold (found by manually thresholding the image on the basis of the infor-

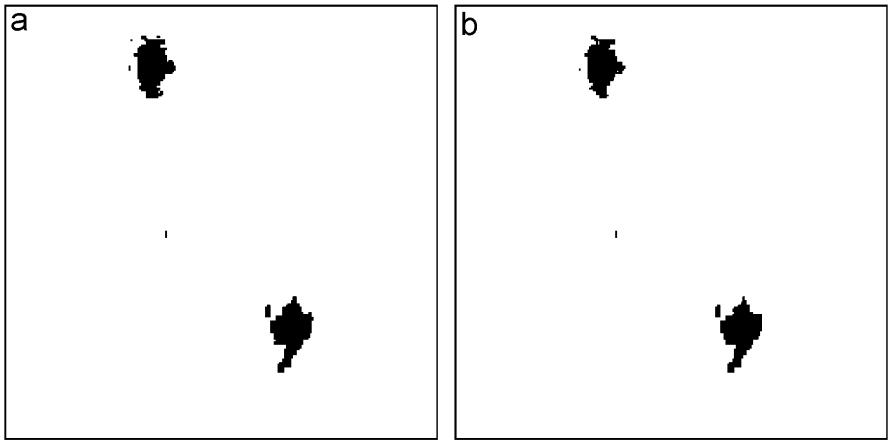

Fig. 9. NDT defective material binary images obtained by: (a) manual supervised optimal thresholding ($t = 156$); (b) the proposed method ($t = 154$).

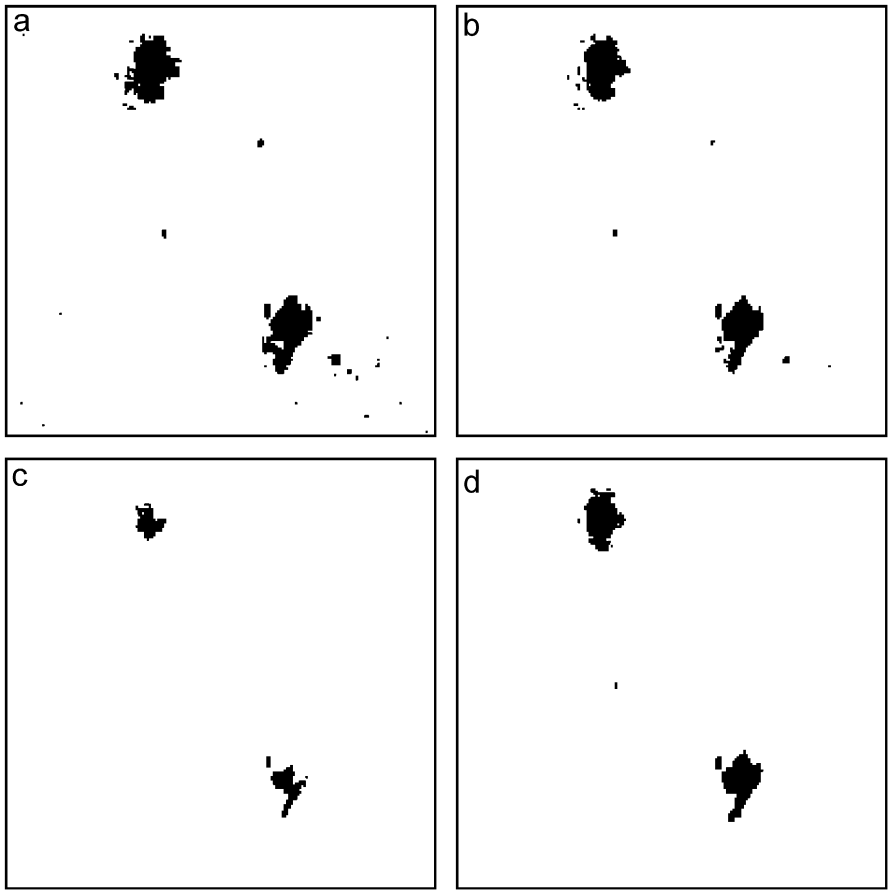

Fig. 10. A comparison for the NDT defective material binary images obtained by the reference thresholding techniques and the proposed method. (a) Entropy-based method ($t = 166$). (b) MET method ($t = 162$). (c) OTSU method ($t = 112$). (d) The proposed method ($t = 156$).

mation present in the ground-truth image) was equal to 170, corresponding to 38 misclassified pixels and its ME equal to 9.5000e − 004 (see Fig. 11 for a visual comparison between the binary image obtained by the proposed method and the one yielded by manual optimal thresholding). Among the reference thresholding techniques, the worst result was provided by entropy-based method (the threshold value was equal to 138, corresponding to 2926 misclassified pixels and its ME equal to 0.0732), which failed to determine a reasonable threshold (the similar result obtained by the OTSU method), while the threshold closest to the one yielded by the proposed method was computed by the MET method (the threshold value was equal to 174, corresponding to 231 misclassified pixels and its ME equal to 0.0058). Fig. 12 gives a visual comparison be-

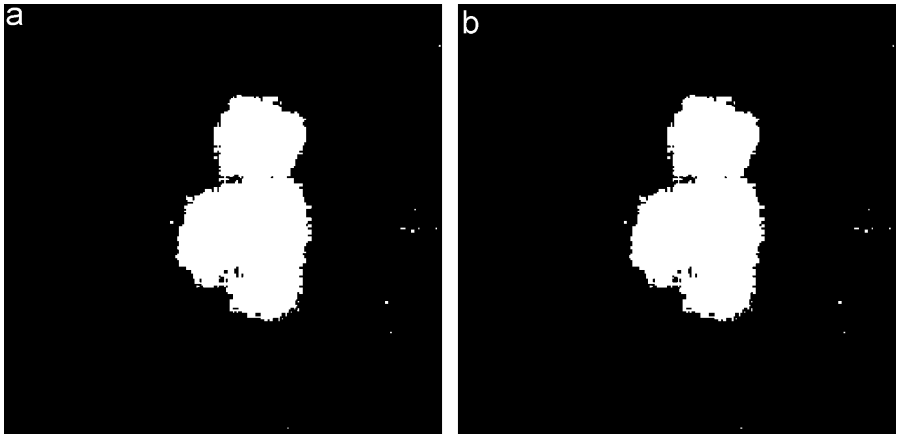

Fig. 11. NDT GFRP images obtained by: (a) manual supervised optimal thresholding ($t = 170$); (b) the proposed method ($t = 171$).

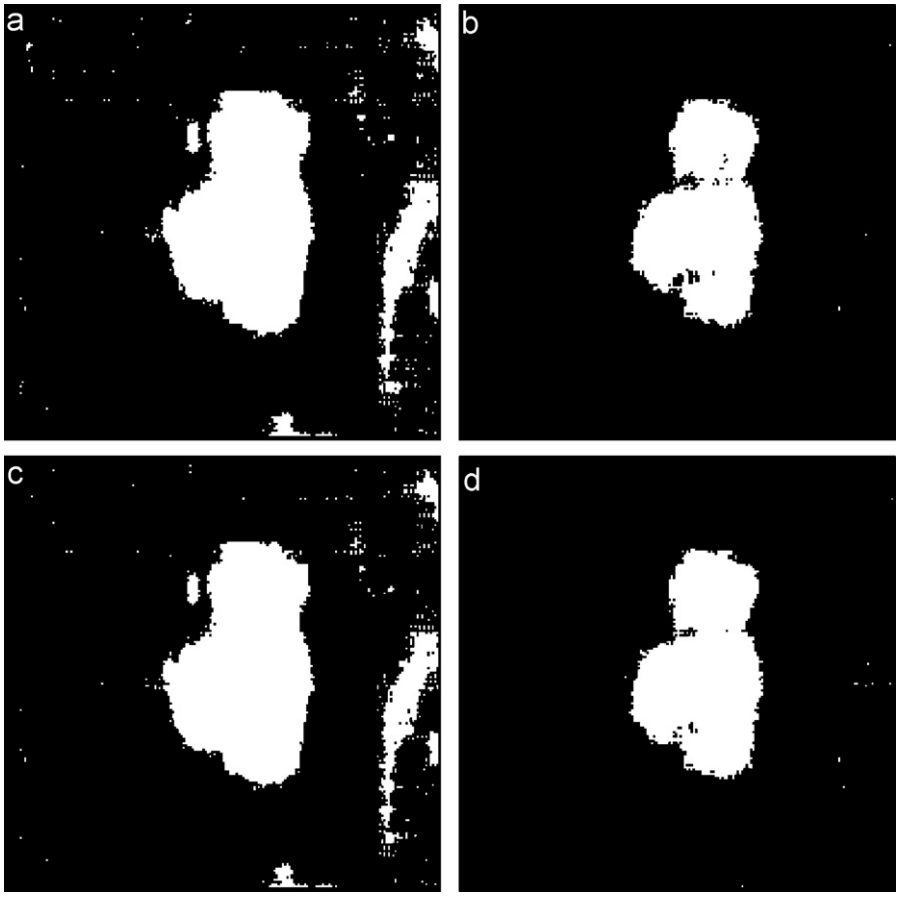

Fig. 12. A comparison for the NDT GFRP binary images obtained by the reference thresholding techniques and the proposed method. (a) Entropy-based method ($t = 138$). (b) MET method ($t = 174$). (c) OTSU method ($t = 140$). (d) The proposed method ($t = 171$).

tween the binary image obtained by the reference thresholding techniques and the proposed method.

4.3. Experiments on other images

In Fig. 13, we show a flower image (see Fig. 13(a)) with an inhomogeneous distribution of light around it, leading to an irregular histogram (see Fig. 13(b)). Fig. 13 presents the thresholding results of the flower image, where the original image together with its histogram and the thresholded images obtained by the reference thresholding techniques and the proposed method are displayed side by side in Fig. 13. From the gray-level histogram, the picture roughly consists of the flower and its background, the probability of the former is much smaller than that of the latter. The MET method yielded threshold 18 which shifts from the valley towards the larger compo-

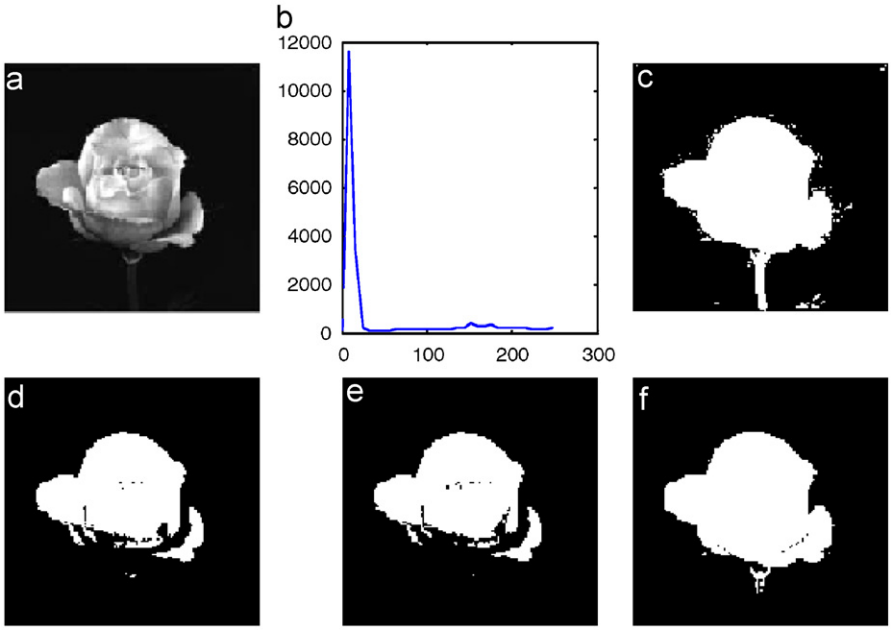

Fig. 13. Flower image, its gray-level histogram and segmentation results.

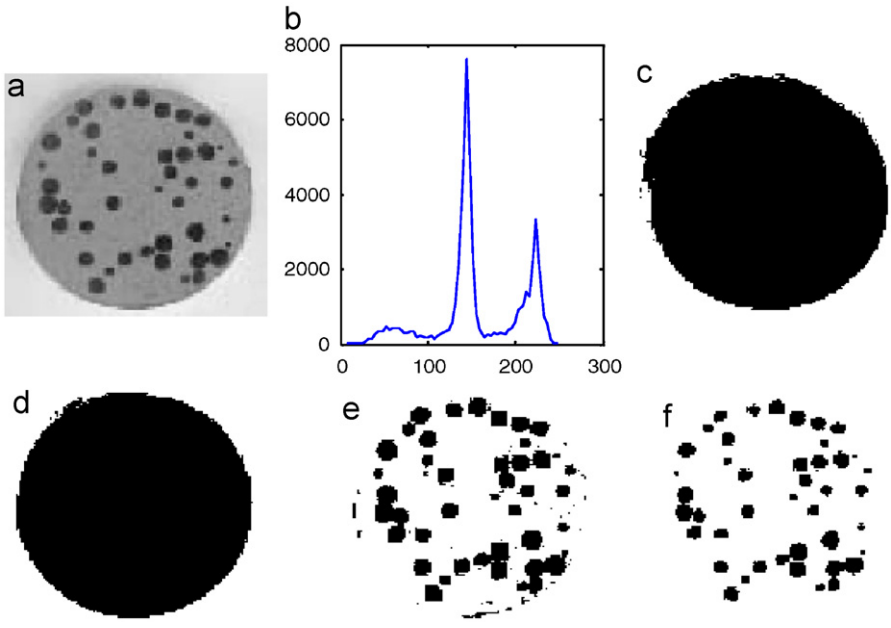

Fig. 14. Shot1 image, its gray-level histogram and segmentation results.

nent. The OTSU method yielded threshold 96 which shifts from the valley towards the smaller component. The entropy-based method yielded threshold 103 which is the same as the OTSU method. Comparatively, the proposed method with threshold (28) is closer to the valley. This observation can also be justified by comparing the thresholded results perceptually. The proposed method is visually better in differentiating the flower from the background. It is also noted that the MET method misclassifies some background as the object. As for the results of both the OTSU method and the entropy-based method, the reported thresholds are evidently far away from the ideal one, which misclassify some objects as the background.

Fig. 14 shows the last example of a shot1 image segmentation. The original image together with its histogram and segmented images obtained by using the MET method, the OTSU method, the entropy-based method and the proposed method here are displayed from (a) to (f) in Fig. 14. From the gray-level histogram (see Fig. 14(b)), the picture roughly consists of three components: the background, the target sheet and the shot dot. In this case, we want to segment the shot dot. The

MET method yielded threshold 204, the OTSU method 174, the entropy-based method 129 and the proposed method 84. As can be seen from the gray-level histogram, both the MET method and the OTSU method yielded large thresholds which are close to the second valley. This leads to the target sheet and the shot dot together as objects (impossible to recognize the position of the shot dot). The entropy-based method and the proposed method seem more acceptable for the segmentation purpose. However, the result of the entropy-based method with threshold 129 which shifts from the valley towards the larger component (the target sheet) leads to misclassifying some background as object. The proposed method is visually better than other methods. This observation can also be justified by comparing the thresholded results perceptually. From Fig. 14(c) to (f), we can see that the thresholded images using the entropy-based method and the OTSU method have a indecent vision which is consistent with the analysis in the above, and the binary image of the proposed method is clearer than that of the entropy-based method.

5. Conclusion

In this paper, we have developed a simple but effective method of image segmentation that employs Parzen window technique. The method effectively combines image histograms information with the spatial information about pixel of different gray levels by using Parzen window technique. The underlying idea of the proposed method is to maximize the difference of spatial probability distribution of the object and background classes. By using the Parzen window technique, the novel criterion function is designed. As we may know well, if there are enough data points in the data space, then Parzen window based estimate can well approximate the unknown probability density function. Generally speaking, an image is very dense (of size $m \times n$!). This fact may perhaps be used to explain why the proposed method here is very effective. Finally, the purpose of this paper is not a commentary on the best global thresholding. Rather, if one decides to use one thresholding method for image segmentation, then it shows that the proposed method here can choose the threshold which is as close to optimal as possible.

Except for the above advantages, our experimental results actually indicate that the high time complexity is the main drawback of the proposed method. In future, as a development of this work, we will optimize the proposed method here to reduce its time complexity, and extend it to the problem of multilevel thresholding.

Acknowledgments

This work is supported by Hong Kong PolyU Grant, National Science Foundation of China, JiangSu Natural Science Foundation (BK2003017), New_century Outstanding Young Scholar Grant of Ministry of Education of China (NCET-04-0496), National 863 Project (Grant No. 2006AA10Z313), National KeySoft Laboratory at Nanjing University, The Key Laboratory of Computer Science at Institute of Software, CAS, China, The Key Laboratory of Computer Information Technologies at JiangSu Province, the 2004 key project of Ministry of Education of China, and National Key Laboratory of Pattern Recognition at Institute of Automation, CAS, China.

References

[1] L. Yang, X. Yang, Multi-object segmentation based on curve evolving and region division, Chin. J. Comput. 27 (3) (2004) 420–425 (in Chinese with English abstract).

[2] Y.J. Zhang, Image Segmentation, Press of Science, Beijing, 2001 (in Chinese).

[3] S. Abutaleb, Automatic thresholding of gray-level pictures using two-dimensional entropies, Pattern Recognition 47 (1989) 22–32.

[4] N. Ahuja, A. Rosenfeld, A note on the use of second order gray-level statistics for threshold selection, IEEE Trans. Systems Man Cybern. 8 (1978) 895–898.

[5] A. Beghdadi, A. Le Negrate, P.V. de Lesegno, Entropic thresholding using a block source model, Graphical Models Image Process. 57 (1995) 197–205.

[6] B. Bhanu, O.D. Faugeras, Segmentation of images having unimodal distribution, IEEE Trans. Pattern Anal. Mach. Intell. 4 (4) (1982) 408–419.

[7] A.D. Brink, Thresholding of digital images using two-dimensional entropies, Pattern Recognition 25 (1992) 803–808.

[8] C. Chang, K. Chen, J. Wang, M.L.G. Althouse, A relative entropy based approach to image thresholding, Pattern Recognition 27 (1994) 1275–1289.

[9] F.J. Chang, J.C. Yen, S. Chang, A new criterion for automatic multilevel thresholding, IEEE Trans. Image Process. 4 (1995) 370–378.

[10] W.T. Chen, C.H. Wen, C.W. Yang, A fast two-dimensional entropic thresholding algorithm, Pattern Recognition 27 (1994) 885–893.

[11] S.C. Cheng, W.H. Tsai, A neural network implementation of the moment-preserving technique and its application to thresholding, IEEE Trans. Comput. 42 (1993) 501–507.

[12] L. Cinque, S. Levialdi, A. Rosenfeld, Fast pyramidal algorithms for image thresholding, Pattern Recognition 28 (1995) 901–906.

[13] L.S. Davis, A. Rosenfeld, J.S. Weszka, Region extraction by averaging and thresholding, IEEE Trans. Systems Man Cybern. 5 (1975) 383–388.

[14] J. Gong, L. Li, W. Chen, Fast recursive algorithms for two-dimensional thresholding, Pattern Recognition 31 (1998) 295–300.

[15] L. Halada, G.A. Ososkov, Histogram concavity analysis by quasicurvature, Comput. Artif. Intell. 6 (1987) 523–533.

[16] L. Hertz, R.W. Schafer, Multilevel thresholding using edge matching, Comput. Vision Graphics Image Process. 44 (1988) 279–295.

[17] L. Huang, M.J. Wang, Image thresholding by minimizing the measures of fuzziness, Pattern Recognition 28 (1995) 41–51.

[18] E.D. Jansing, T.A. Albert, D.L. Chenoweth, Two-dimensional entropic segmentation, Pattern Recognition Lett. 20 (1999) 329–336.

[19] G. Johannsen, J. Bille, A threshold selection method using information measures, in: Proceedings of the Sixth International Conference on Pattern Recognition, Munich, Germany, 1982.

[20] J.N. Kapur, P.K. Sahoo, A.K.C. Wong, A new method for gray level picture thresholding using the entropy of the histogram, Comput. Vision Graphics Image Process. 29 (1985) 273–285.

[21] R.L. Kirby, A. Rosenfeld, A note on the use of (gray level, local average gray level) space as an aid in threshold selection, IEEE Trans. Systems Man Cybern. 9 (1979) 860–864.

[22] T. Kurita, N. Otsu, N. Abdelmalek, Maximum likelihood thresholding based on population mixture models, Pattern Recognition 25 (1992) 1231–1240.

[23] N. Otus, A threshold selection method from gray-level histograms, IEEE Trans. Systems Man Cybern. 9 (1979) 62–66.

[24] J. Kittler, J. Illingworth, Minimum error thresholding, Pattern Recognition 19 (1) (1986) 41–47.
[25] J.N. Kapur, P.K. Sahoo, A. Wong, A new method for gray-level picture thresholding using the entropy of the histogram, Comput. Vision Graphics Image Process. 29 (1985) 273–285.
[26] S. Abutaleb, Automatic thresholding of gray-level picture using two-dimensional entropy, Comput. Vision Graphics Image Process. 47 (1989) 22–32.
[27] M. Portes de Albuquerque, I.A. Esquef, A.R. Gesualdi Mello, M. Portes de Albuquerque, Image thresholding using Tsallis entropy, Pattern Recognition Lett. 25 (2004) 1059–1065.
[28] P.K. Saha, J.K. Udupa, Optimum image thresholding via class uncertainty and region homogeneity, IEEE Trans. Pattern Anal. Mach. Intell. 23 (7) (2001) 689–706.
[29] Z.Q. Bian, X.G. Zhang, Pattern Recognition, second ed., Tsinghua University Press, Beijing, 2000.
[30] R.O. Duda, P.E. Hart, D.G. Stork, Pattern Classification, (H.D. Li, T.X. Yao, Trans.), Machinery Industry Press, Beijing, 2003.
[31] K. Torkkola, Feature extraction by non-parametric mutual information maximization, J. Mach. Learn. Res. 3 (2003) 1415–1438.
[32] P.K. Sahoo, G. Arora, A thresholding method based on two-dimensional Renyi's entropy, Pattern Recognition Lett. 37 (2004) 1149–1161.
[33] S. Wang, F.L. Chung, Note on the equivalence relationship between Renyi-entropy based and Tsallis-entropy based image thresholding, Pattern Recognition Lett. 26 (14) (2005) 2309–2312.
[34] M. Sezgin, B. Sankur, Survey over image thresholding techniques and quantitative performance evaluation, J. Electron. Imaging 13 (1) (2004) 146–165.
[35] W.A. Yasnoff, J.K. Mui, J.W. Bacus, Error measures for scene segmentation, Pattern Recognition 9 (1997) 217–231.
[36] Y.J. Zhang, A survey on evaluation methods for image segmentation, Pattern Recognition 29 (1996) 1335–1346.
[37] Y. Bazi, L. Bruzzone, F. Melgani, Image thresholding based on the EM algorithm and generalized Gaussian distribution, Pattern Recognition 40 (2007) 619–634.
[38] Z. Hou, Q. Hu, W.L. Nowinski, On minimum variance thresholding, Pattern Recognition Lett. 27 (2006) 1732–1743.
[39] R.R. Roldan, J.F.G. Lopera, C.A. Alloah, et al., A measure of quality for evaluating methods of segmentation and edge detection, Pattern Recognition 34 (2001) 969–980.

About the Author—WANG SHITONG received the M.S. degree in computer science from Nanjing University of Aeronautics and Astronautics, China, in 1987. He visited London University and Bristol University in UK, Hiroshima International University in Japan, Hong Kong University of Science and Technology, Hong Kong Polytechnic University, and Hong Kong City University in Hong Kong, as a Research Scientist, for over four years. Since 2000, he is a Full Professor in the School of Information of Southern Yangtse University, China. His research interests include AI, neuron-fuzzy systems, pattern recognition, and image processing. He has published about 80 papers in international/national journals and has authored seven books.

About the Author—FU-LAI CHUNG received the B.Sc. degree from the University of Manitoba, Canada, in 1987, and the M.Phil. and Ph.D. degrees from the Chinese University of Hong Kong, in 1991 and 1995, respectively. He joined the Department of Computing, Hong Kong Polytechnic University, in 1994, where he is currently an Associate Professor. He has published widely in the areas of fuzzy systems, neural networks, and pattern recognition. His current research interests include fuzzy data mining, fuzzy neural network modeling, and fuzzy techniques for multimedia applications.

About the Author—FUSONG XIONG is a postgraduate student now. His research interests include pattern recognition, bioinformatics and their applications.